



Synthesis, X-ray diffraction study and pharmacological evaluation of 3-amino-4-methylthiophene-2-acylcarbohydrazones

SONJA HERRMANN^{1,3}, TABEA SCHÜBEL^{1,3}, FANNY N. COSTA², MARIA LETÍCIA C. BARBOSA¹,
FABIO F. FERREIRA², THAYS L.M.F. DIAS⁴, MORGANA V. ARAÚJO⁴, MAGNA S. ALEXANDRE-
MOREIRA⁴, LÍDIA M. LIMA¹, STEFAN LAUFER³ and ELIEZER J. BARREIRO¹

¹Laboratório de Avaliação e Síntese de Substâncias Bioativas/LASSBio[®], Universidade Federal do Rio de Janeiro/UFRJ, Av. Carlos Chagas Filho, 373, Caixa Postal 68024, 21944-971 Rio de Janeiro, RJ, Brazil

²Centro de Ciências Naturais e Humanas/CCNH, Universidade Federal do ABC/UFABC, Av. dos Estados, 5001, 09210-580 Santo André, SP, Brazil

³Department of Pharmaceutical/Medicinal Chemistry, Institute of Pharmacy, Eberhard-Karls-University Tübingen, Av. Auf der Morgenstelle, 8, D-72076 Tübingen, Germany

⁴Laboratório de Farmacologia e Imunidade/LaFI, Instituto de Ciências Biológicas e da Saúde, Universidade Federal de Alagoas/UFAL, Av. Lourival Melo Mota, s/n, Cidade Universitária, 57020-720 Maceió, AL, Brazil

Manuscript received on October 8, 2017; accepted for publication on October 30, 2017

ABSTRACT

N-acylhydrazone is an interesting privileged structure that has been used in the molecular design of a myriad of bioactive compounds. In order to identify new antinociceptive drug candidates, we described herein the design, synthesis, X-ray diffraction study and the pharmacological evaluation of a series of 3-amino-4-methylthiophene-2-acylcarbohydrazone derivatives (**8a-t**). Compounds were prepared in good overall yields through divergent synthesis from a common key intermediate and were characterized by classical spectroscopy methods. X-ray diffraction study was employed for unequivocal determination of the imine double bond stereochemistry. **8a-t** were evaluated *in vivo* through oral administration using the classical writhing test in mice. *N*-acylhydrazone derivatives **8j** and **8l** displayed relative potency similar to dipyrone, highlighting them as promising analgesic lead-candidates for further investigation.

Key words: *N*-acylhydrazone, privileged structure, antinociceptive, p38MAPK, X-ray.

INTRODUCTION

The original definition of a privileged scaffold dates back to the year 1988 and was first described

by Evans and coworkers (Evans et al. 1988). This concept refers to a single molecular framework, correlated to a minimum structural subunit, which affects more than one bioreceptor or enzyme target. The adequate functionalization allows the modulation of the different biological activities and of the selectivity. Rational employment of molecular modification strategies, such as molecular hybridization, bioisosterism, molecular simplification, homologation and conformational

Correspondence to: Stefan Laufer
E-mail: stefan.laufer@uni-tuebingen.de
Eliezer J. Barreiro
E-mail: ejbarreiro@ccsdecania.ufrj.br

* Contribution to the centenary of the Brazilian Academy of Sciences.

restriction are applied to adapt and adjust the selected scaffold to the desired pharmacological application. These structural modifications lead to different patterns of lipophilic/hydrophilic nature, H-bonding donor/acceptor properties, electron donating/withdrawing profile, acid/basic character and conformational behavior of the pharmacophoric groups. On the other hand, the previously described synthetic accessibility and the possibility of rational modifications offer access to a wide range of applications for these molecular frameworks, representing an opportunity for rapid, economic and optimized discovery of new drug candidates (Duarte et al. 2007, Evans et al. 1988, Jones 2017).

A well-known example of a privileged structure is the imidazole scaffold. This heterocyclic ring is found in bioactive compounds affecting a wide range of targets, *e.g.* cimetidine, a H1-receptor antagonist; losartan, an AT1-receptor antagonist; clotrimazole, an antifungal agent; metronidazole, an antimicrobial drug; mercaptopurine, a purine nucleoside antimetabolite; and theophylline, a nonselective phosphodiesterase inhibitor and nonselective adenosine receptor antagonist (Duarte et al. 2007).

Lately, the N-acylhydrazone (NAH; Figure 1) scaffold has been also described as an interesting privileged structure. This chemical framework has been used in the design of several bioactive compounds for treatment of infections (Gu et al. 2012, He et al. 2017, Hernández et al. 2013, Jin et al. 2010, Palace-Berl et al. 2013), schizophrenia (Cutshall et al. 2012, Gage et al. 2011), cancer (Abdel-Aziz et al. 2012, de Figueiredo et al. 2017, Zhai et al. 2013), hypertension (Kümmerle et al. 2009), diabetes (Hernández-Vázquez et al. 2016), nociception and inflammatory disorders (Azizian et al. 2016, Jagtap et al. 2011, Khalil et al. 2013, Ozadali et al. 2012, Ünsal-Tan et al. 2010). The biological versatility of the NAH moiety and its easy synthetic accessibility make it a simple

and unique privileged scaffold to be explored in Medicinal Chemistry (Duarte et al. 2007).

Among the biological activities described for NAH derivatives, the analgesic and anti-inflammatory properties are noteworthy. Several NAH compounds are well-known inhibitors of relevant inflammation targets, including cyclooxygenases (COX) (Gundogdu-Hizliates et al. 2014, Ünsal-Tan et al. 2010), inducible nitric oxide synthase (iNOS) (Moldovan et al. 2011, Tipericiuc et al. 2013) and the p38 mitogen-activated protein kinase (p38 MAPK) (Lacerda et al. 2012). Examples of promising analgesic and anti-inflammatory NAH lead candidates (**1-7**) are depicted in Figure 1, highlighting the 3-aminothiophene-2-acylhydrazone derivatives (**7a** and **7b**), which have recently been described by our research group as non-toxic, analgesic and anti-inflammatory candidates (Da Silva et al. 2014).

We described herein the synthesis, X-ray diffraction study and *in vivo* and *in vitro* pharmacological evaluation of new 3-amino-4-methylthiophene-2-acylcarbohydrazones (**8a-t**), designed by the introduction of a methyl group at position 4 of the thiophene ring in order to explore the methylation effect (Barreiro et al. 2011) in the biological profile of this new series of NAH derivatives (Figure 2). Moreover, the design concept explored the possibility to employ the same starting material used in the synthesis of the local anesthetic articaine (*i.e.* methyl 3-amino-4-methylthiophene-2-carboxylate, **9**) (Li et al. 2013), already known as a safe structural framework, contributing to the synthetic accessibility and drug-like properties of the NAHs (**8a-t**) described here.

MATERIALS AND METHODS

CHEMISTRY

All commercially available reagents and solvents were used without further purification. Reactions were routinely monitored by thin-

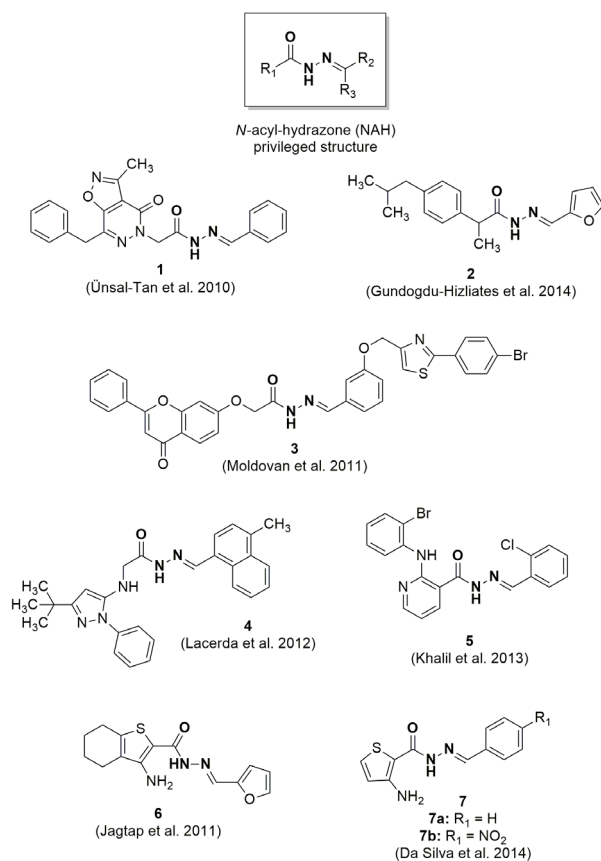


Figure 1 - Analgesic and anti-inflammatory drug candidates presenting the privileged *N*-acyl-hydrazone (NAH) structure.

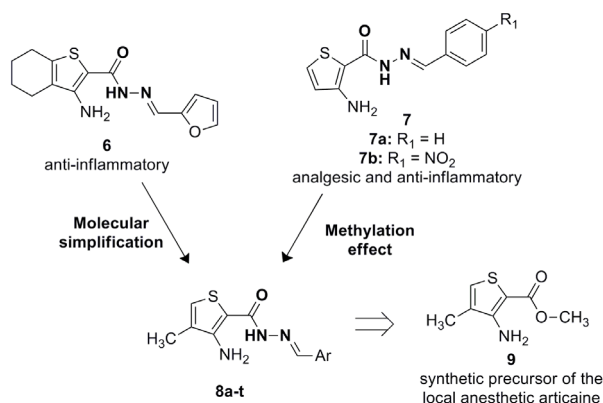


Figure 2 - Design concept of the *N*-acyl-hydrazone (NAH) derivatives (**8a-t**).

layer chromatography (TLC) in silica gel plates (KieselGel 60 F254 Merck). The mobile phase consisted of a mixture of 70% hexane/30% ethyl acetate or 95% dichloromethane/5% methanol. The developed plates were examined with UV lamps (in wavelength of 254 nm and 365 nm) or by employing the color reagents iodine, 2,4-dinitrophenylhydrazine (coloring ketones or aldehydes) or 4-dimethylaminobenzaldehyde (highlighting amines). The melting points (m.p.) of the final products were determined by differential scanning calorimetry (DSC) using a Shimadzu DSC-60, with a heating rate of 20 °C/min and a maximum temperature of 300 °C. The results were recorded as the onset temperatures (Tonset), which are defined as the point of intersection of the tangent of the peak with the extrapolated baseline. The apparatus DSC-60 was calibrated with indium (In, m.p. 157 °C).

Mass spectrometry (MS) was performed by positive ionization at Bruker Amazon SL. EI-ion-trap MS (electrospray ionization ion trap mass spectrometry) and the data were analyzed by Compass 4.0 software. The relative purity of the final compounds (**8a-t**) was determined by high performance liquid chromatography (HPLC) using a Shimadzu apparatus- LC20AD, column Kromasil 100-5 C18 (4.6 mm x 250 mm) and detector SPD-M20A (Diode Array) in the substance-specific wavelength (240-370 nm), employing a constant flux of 1 mL/min with an injection volume of 20 µL. A mixture of 70% methanol/30% water (A) or 80% methanol/20% water (B) was used as solvent. Standard HPLC solvents were purchased from TEDIA®. Data were acquired by software “LC solution” version 4.0. Infrared (IR) spectra were obtained using a Thermo Nicolet IS 10 FT-IR spectrometer equipped with smart iTR ATR accessory for direct measurements.

The ¹H and ¹³C nuclear magnetic resonance spectra were determined in DMSO-*d*₆ solutions using a Bruker AC-200 spectrometer with 200

MHz for ^1H and 50 MHz for ^{13}C (LABRMN, UFRJ). The chemical shifts are given in parts per million (δ) from solvent residual peaks and the coupling constant values (J) are given in Hz. Signal multiplicities are represented by: s (singlet), d (doublet), t (triplet) and m (multiplet). The synthetic methodologies and the detailed structure analysis for the target compounds (**8a-t**) are described in the Experimental Section.

X-RAY DIFFRACTION STUDY

In order to obtain a good X-ray powder diffraction (XRPD) pattern, the sample preparation is an important step. The selected compound **8j** was gently hand-grinded using a pestle and an agate mortar. The measurement was carried out at room temperature on a STADI-P powder diffractometer (Stoe[®], Darmstadt, Germany) using transmission geometry with $\text{CuK}_{\alpha 1}$ ($\lambda = 1.54056 \text{ \AA}$) radiation. The wavelength was selected by a curved Ge (111) crystal, with a tube voltage of 40 kV and a current of 40 mA. The fine powdered sample was loaded into a 0.3 mm diameter special glass capillary nr. 14 (Hilgenberg[®], Malsfeld, Germany), which was kept spinning during data collection. A Mythen 1K (Dectris[®], Baden, Switzerland) linear detector was used and the reflections were detected in the range from 3° to 61.785° , with step sizes of 0.015° and 600 s of integration time at each 1.05° .

On the basis of previous procedures (Costa et al. 2015, 2013), the crystal structure of **8j** was determined using the DASH software program (David et al. 2006). *Topas-Academic v.5* (Coelho et al. 2011) was used to index the diffraction pattern as well as to refine the crystal structure.

BIOLOGICAL ASSAYS

Acetic acid-induced writhing test

Nociception was induced by the i.p. injection of acetic acid (0.6%, v/v; 0.1 mL/10g body weight).

The number of writhes, a response consisting of the contraction of the abdominal wall and pelvic rotation, followed by hind-limb extension, was counted during continuous observation for 20 min, beginning 5 min after the acetic acid injection. NAH derivatives **8a-t** (100 $\mu\text{mol/kg}$, oral administration) were administered 40 min before the acetic acid injection. The control group received 10 mL/kg of the vehicle (distilled water with 20 μL of Tween 80) via the i.p. route. Antinociceptive activity was expressed as percentage of inhibition of the usual number of writhing observed in control animals (Collier et al. 1968). The Research Ethics Committee from the Federal University of Alagoas (UFAL) approved the animal experimental model presented in this study and the process protocol number is n^o 55/2013.

p38 MAPK inhibition assay

The experimental settings and screening procedures of the employed nonradioactive immunosorbent p38 α mitogen-activated protein kinase (p38 α MAPK) activity assay have previously been described (Goettert et al. 2010). The ELISA assay was performed using 96-well plates (Nunc MaxiSorp[®], Fisher Scientific), which were coated with 50 μL /well (10 $\mu\text{g/mL}$) in Tris-buffered saline (TBS) of the p38 α substrate ATF-2 (ProQinase, Freiburg, Germany) and stored overnight at 4°C . Subsequently, each plate was washed three times with bi-distilled water and remaining binding sites were blocked with blocking buffer (BB: 0.05 % Tween 20, 0.025 % bovine serum albumin (BSA) and 0.02 % NaN_3 in TBS) for 30 minutes at room temperature and washed again three times. A 10 mM stock solution of samples was prepared in dimethyl sulfoxide and further diluted in a kinase buffer (KB), which contained 12 ng/50 μL activated p38 α MAPK (Prof. Dr. J. Schultz, University of Tübingen, Germany), 50 mM Tris of pH 7.5, 10 mM MgCl_2 , 10 mM β -Glycerolphosphate, 100 $\mu\text{g/}$

mL BSA, 1 mM Dithiothreitol, 0.1 mM Na_3VO_4 , and 100 μM ATP were used to dilute the samples and as control. 50 μL of each dilution (0.01-10 μM) was pipetted into the corresponding wells and incubated 1 hour at 37 °C. After washing this dilution three times with bi-distilled water, blocking it for 15 minutes and washing it three more times, the 50 μL of diluted monoclonal anti-phospho-ATF-2 (Thyr69/71) peroxidase-conjugated antibody (1:5000) (Sigma, Germany) in blocking buffer adjusted to a pH of 6.5 was added into each well and incubated for 1 hour at 37 °C, followed by adding 50 μL of 3,3',5,5'-tetramethylbenzidine (TMB) (BD Bioscience, Europe) substrate into all wells. Then, the peroxide-labeled conjugates developed a definitive blue color, which was measured photometrically at 650 nm or was read at 450 nm with an ELISA reader (SOFTmax PRO software) after stopping with 25 μL of 2 N H_2SO_4 . The inhibitor SB 203580 (Laboratory Prof. Dr. S.A. Laufer, University of Tübingen, Germany) was used as reference.

RESULTS AND DISCUSSION

CHEMISTRY

The designed 3-amino-4-methylthiophene-2-acylcarbohydrazones (**8a-t**) were synthesized efficiently via divergent synthesis as outlined in Figure 3. Starting from the synthetic precursor methyl 3-amino-4-methylthiophene-2-carboxylate (**9**), the key intermediate 3-amino-4-methylthiophene-2-carbohydrazide (**10**) was prepared by hydrazinolysis reaction. With intermediate **10** in hands, the NAH derivatives **8a-t** were obtained by classical condensation with functionalized aldehydes under acid catalysis (Da Silva et al. 2014, Lacerda et al. 2012). The target compounds (**8a-t**) were prepared in good yields, between 42.4 and 95.5%, and were analyzed by HPLC, MS, IR, $^1\text{H-NMR}$ and $^{13}\text{C-NMR}$. Analytical

data were in full agreement with the proposed structures.

It's relevant to mention that NAHs may exist as *E/Z* geometrical isomers regarding the $-\text{C}=\text{N}$ -double bond configuration, and may be observed as *cis/trans* amide ($-\text{CO-NH-}$) conformers (Abdel-Aziz et al. 2012, Khalil et al. 2013). To address this subject a careful analysis of the $^1\text{H-NMR}$ signals recorded for compounds **8a-t** in $\text{DMSO-}d_6$ was conducted. Only one single signal related to the imine hydrogen ($\text{CH}=\text{N}$) was detected, with chemical displacement varying between 7.81 ppm and 8.21 ppm. These data indicate that the NAH derivatives **8a-t** were synthesized in just one geometrical isomer. Based on chemical shifts of *E/Z*-isomer reported in literature (Palla et al. 1982), compounds **8a-t** were assumed to have the *E* configuration for their imine double bond. To confirm this assumption, XRPD studies were performed using compound **8j** as a model. As depicted in Figure 4, the crystal structure of **8j** is arranged in a monoclinic space group (*Cc*), with unit cell dimensions $a = 38.971(6)$ Å, $b = 4.8314(6)$ Å, $c = 18.843(2)$ Å, $\beta = 109.964(4)$ ° and $V = 3334.6(8)$ Å³. The goodness of fit indicator and *R*-factors were, respectively: $\chi^2 = 3.153$, $R_{\text{exp}} = 1.166\%$, $R_{\text{wp}} = 3.675\%$ and $R_{\text{Bragg}} = 2.945\%$. The crystal structure of compound **8j** is comprised by eight formula units per unit cell ($Z = 8$), accommodating two molecules in the asymmetric unit ($Z' = 2$). The relative configuration *E* about the imine double bond was observed, corroborating with the assignment based on NMR shifts. Regarding the conformation of the amide subunit (CONH), X-ray powder diffraction studies revealed a *cis*-conformation in the crystal structure of **8j**. The hydrogen inter/intramolecular interactions contribute to the organization of the space arrangement in the unit cell. The intermolecular interactions can be observed between atoms $\text{N}(9)-\text{H}(55)\cdots\text{O}(34)$ ($\text{D-H} = 0.9$ Å, $\text{H}\cdots\text{A} = 2.4$ Å, $\text{D}\cdots\text{A} = 3.2$ Å and $\text{D-H}\cdots\text{A} = 144^\circ$) and $\text{N}(33)-$

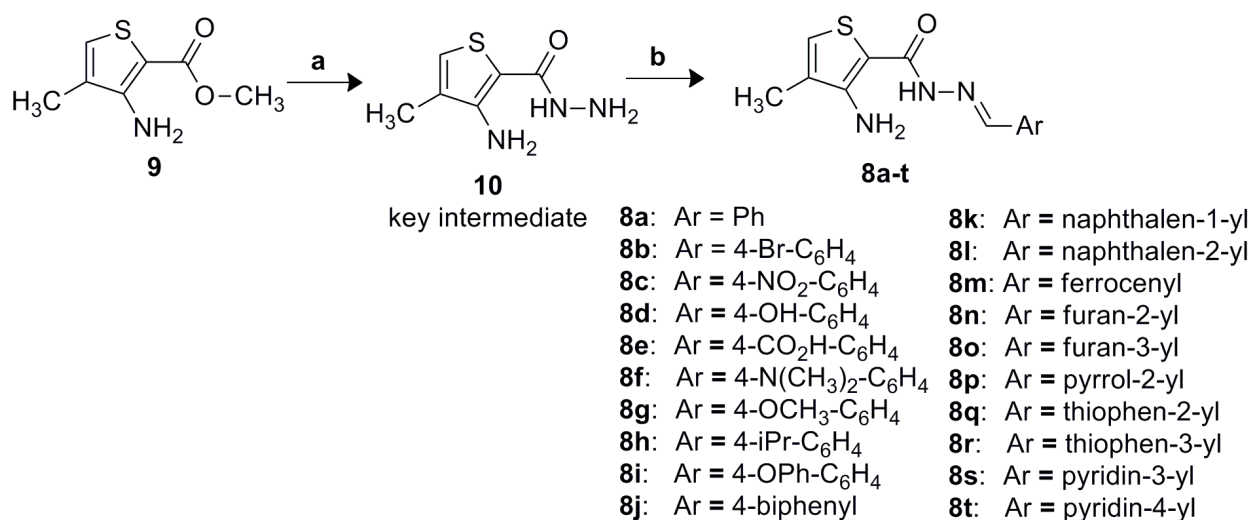


Figure 3 - General methodology for synthesis of 3-amino-4-methylthiophene-2-acylcarbohydrazones **8a-t**. Reagents and Conditions: **a**) N₂H₄·H₂O (80%), EtOH, 80 °C, reflux, 80 h, 74.1%; **b**) ArCHO, EtOH, HCl (cat), r.t., 0.5-3.5 h, 42.4-95.5%.

H(72)···O(10) (D–H = 0.9 Å, H···A = 2.3 Å, D···A = 3.1 Å and D–H···A = 147°), where “D” and “A” are, respectively, hydrogen donor and acceptor. For the intramolecular interactions the involved atoms are N(4)–H(49)···O(10) (D–H = 0.9 Å, H···A = 2.1 Å, D···A = 2.7 Å and D–H···A = 133°) and N(28)–H(66)···O(34) with a distance D–H = 0.9 Å, H···A = 2.0 Å, D···A = 2.7 Å and D–H···A = 129°. All interactions are represented by cyan lines in Fig. 4. Supplementary crystallographic data can be found on the Cambridge Crystallographic Data Centre web site (www.ccdc.cam.ac.uk/data_request/cif) searching for CCDC ID: 1576495.

PHARMACOLOGICAL EVALUATION

Considering the previously described analgesic and anti-inflammatory properties of 3-aminothiophene-2-acylhydrazones **7a** and **7b** (Da Silva et al. 2014), we decided in a first approach to study the antinociceptive profiles of the methylated analogues **8a-t** using the classical writhing test. In this animal model, peripheral pain is induced in mice by a parenteral administration of acetic acid. Consequently, signals are sent to the central nervous system, causing release of several mediators, including prostaglandins, which

contribute to increased sensitivity of nociceptors. As summarized in Table I, the 3-amino-4-methylthiophene-2-acylcarbohydrazones **8a-t** were evaluated in a screening dose of 100 µmol/kg by oral administration, using dipyrone as standard.

Among all evaluated compounds, ten derivatives (**8b**, **8c**, **8d**, **8f**, **8h**, **8i**, **8m**, **8p**, **8s** and **8t**) were inactive in comparison to control, not being able to reduce the amount of constrictions. **8e**, **8o** and **8r** presented weak inhibitory activity, whereas **8a**, **8g**, **8k**, **8n** and **8q** showed moderate antinociceptive effect at this dose. Explicitly, two derivatives (**8j** and **8l**) demonstrated an expressive antinociceptive activity at the evaluated dose, with 70.0% and 70.2% of inhibition, comparable to the inhibition found for the standard dipyrone.

In comparison to the non-methylated original analgesic and anti-inflammatory prototypes **7a** (Ar = phenyl; ID₅₀ = 3,5 µmol/kg in acetic acid-induced writhing model, p.o.) and **7b** (Ar = 4-nitro-phenyl; ID₅₀ = 2,6 µmol/kg in acetic acid-induced writhing model, p.o.) (Da Silva et al. 2014), the methylation effect was deleterious for the antinociceptive profile of the methylated counterparts **8a** (Ar = phenyl) and **8c** (Ar = 4-nitro-phenyl). On the other hand, regarding the aromatic ring linked to the imine

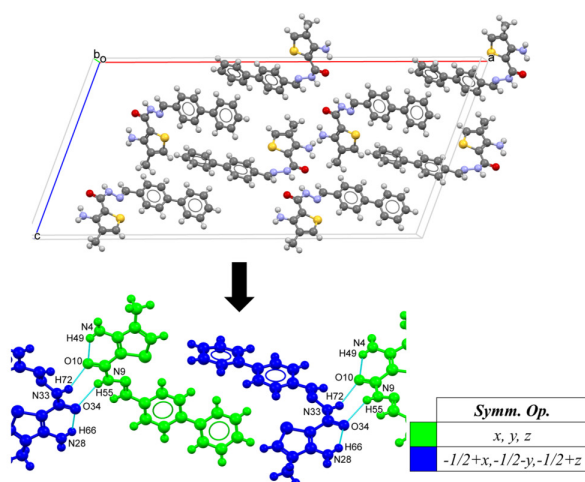


Figure 4 - (Top) Unit cell representation of compound **8j** recognized by X-ray powder diffraction. (Bottom) The hydrogen inter/intramolecular interactions between the atoms from different equivalent symmetry operations are displayed in cyan lines.

carbon, the introduction of more hydrophobic and bulky aromatic systems such as 4-biphenyl (**8j**) and 2-naphthyl (**8l**), not yet explored for the previously described 3-aminothiophene-2-acylhydrazones, proved to be useful for the optimization of the antinociceptive effect within the series.

Particularly, the p38 mitogen-activated protein kinase (p38 MAPK) plays a key role in inflammatory disorders, and it has been also implicated in the signal transduction cascade associated with chronic nociception and nociceptive sensitization (Anand et al. 2011, Lin et al. 2014, Zarubin and Han 2005). Our research group already described novel NAH derivatives designed as p38 MAPK inhibitors as orally active anti-inflammatory and antinociceptive drug candidates (Lacerda et al. 2012). Therefore, we also investigated the ability of compounds **8a-t** to inhibit the enzymatic activity of p38 α MAPK, using a nonradioactive immunosorbent assay and SB203590 as standard. As depicted in Table I, at the screening concentration of 10 μ M, NAH derivatives **8a-t** revealed weak p38 α inhibition or were totally inactive. Although compounds **8a**, **8d**, **8m**, **8q**, **8s** and **8t** presented inhibitory percentages above

30%, none of the investigated NAH derivatives reached an inhibitory effect of 50%, indicating IC₅₀ values above the tested concentration of 10 μ M. Moreover, no correlation was observed between the *in vivo* antinociceptive activities and the *in vitro* p38 MAPK inhibitory effect, indicating that this protein kinase is not the main biological target of the 3-amino-4-methylthiophene-2-acylcarbohydrazone bioactive analogues, mainly **8j** and **8l**.

CONCLUSIONS

In an attempt to identify new antinociceptive drug candidates, twenty 3-amino-4-methylthiophene-2-acylcarbohydrazones (**8a-t**) were synthesized in good overall yields and, based on X-ray powder diffraction studies realized with compound **8j**, the relative configuration of their imine double bond was elucidated. Moreover, these studies revealed a *cis*-conformation for the amide subunit in the crystal structure of **8j**. The compounds described herein were overall less potent than the non-methylated original series, with exception of the new NAH derivatives **8j** and **8l**, which displayed relative potency similar to dipyrone, a traditional analgesic used worldwide for the treatment of acute and chronic pain. These results suggest that the introduction of more hydrophobic and bulky aromatic systems linked to the imine carbon, such as 4-biphenyl (**8j**) and 2-naphthyl (**8l**), represents a favorable structural modification for optimization of the antinociceptive effect within the described series.

EXPERIMENTAL SECTION

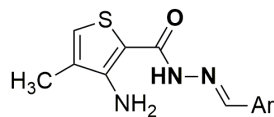
SYNTHESIS AND CHARACTERIZATION OF COMPOUNDS

Synthesis of the key intermediate (3-amino-4-methylthiophene-2-carbohydrazone, 10)

In a 100 mL flask equipped with a magnetic stirrer and a reflux condenser, methyl 3-amino-4-

TABLE I

Effect of the target compounds (8a-t) and dipyrone (100 $\mu\text{mol/kg}$; p.o.) on the 0.6% acetic acid-induced abdominal constriction model in mice (period of 25 min), and, in the last column, percentage of inhibition of p38 α MAPK enzymatic activity for the compounds (8a-t) and positive standard SB-203580 (10 μM) in the nonradioactive immunosorbent assay.



8a-t

| Compound | Abdominal constrictions | | P38 α MAPK |
|-----------|---|------------------------------|-------------------|
| | (Mean \pm S.E.M.) | Percentage of Inhibition [%] | Inhibition [%] |
| Control | 28.9 \pm 2.3 | - | - |
| Dipyrone | 8.0 \pm 2.4 | 70.2** | - |
| SB 203580 | - | - | 92.1 |
| 8a | Ph | 15.2 \pm 2.2 | 47.4** |
| 8b | 4-Br-C ₆ H ₄ | 23.4 \pm 6.9 | - |
| 8c | 4-NO ₂ -C ₆ H ₄ | 25.8 \pm 4.2 | - |
| 8d | 4-OH-C ₆ H ₄ | 28.7 \pm 5.2 | - |
| 8e | 4-CO ₂ H-C ₆ H ₄ | 16.0 \pm 2.9 | 40.5* |
| 8f | 4-[N(CH ₃) ₂]-C ₆ H ₄ | 26.7 \pm 2.2 | - |
| 8g | 4-OCH ₃ -C ₆ H ₄ | 13.0 \pm 6.2 | 55.0** |
| 8h | 4-iPr-C ₆ H ₄ | 30.6 \pm 5.2 | - |
| 8i | 4-OPh-C ₆ H ₄ | 26.0 \pm 3.3 | - |
| 8j | 4-biphenyl | 8.8 \pm 3.5 | 70.0*** |
| 8k | naphthalen-1-yl | 12.8 \pm 3.5 | 55.7** |
| 8l | naphthalen-2-yl | 8.6 \pm 6.1 | 70.2*** |
| 8m | Ferrocenyl | 25.5 \pm 5.4 | - |
| 8n | furan-2-yl | 12.2 \pm 2.3 | 57.9** |
| 8o | furan-3-yl | 19.0 \pm 1.8 | 34.3* |
| 8p | pyrrol-2-yl | 25.0 \pm 1.9 | - |
| 8q | thiophen-2-yl | 11.0 \pm 5.8 | 61.9** |
| 8r | thiophen-3-yl | 16.7 \pm 5.0 | 42.2* |
| 8s | pyridin-3-yl | 21.4 \pm 2.9 | - |
| 8t | pyridin-4-yl | 27.0 \pm 3.8 | - |

Data are expressed as mean \pm S.E.M. Statistical differences between the treated and the control group were evaluated by ANOVA and Dunnett tests; the asterisks denote the levels of significance in comparison with control groups. *p < 0.05; **p < 0.01; ***p < 0.001.

methylthiophene-2-carboxylate (**9**) (1.02 g; 5.96 mmol) was dissolved in absolute ethanol (10.0 mL) and heated at 80 °C. Afterwards, an 80% solution of hydrazine monohydrate (9.36 g; 3.07 mL; 292 mmol) was slowly added to the reaction medium, which was constantly stirred at 80°C. The reaction mixture was maintained under reflux for 80 hours,

at which time TLC (70% hexane/30% ethyl acetate; 4-dimethylaminobenzaldehyde) indicated the end of the reaction. After cooling, reaction media was concentrated under reduced pressure. By adding crushed ice to the flask, the desired carbohydrazide (**10**) precipitated as yellow crystalline solid and was collected by vacuum filtration. The key

intermediate **10** was collected with a yield of 74.1 %. The ^1H NMR and ^{13}C NMR data for compound **10** are consistent with previous reports (Al-Nuri and Husein 2011).

General procedure for synthesis of target compounds 8a-t

In a 50 mL flask equipped with a magnetic stirrer, 3-amino-4-methylthiophene-2-carbohydrazide (**10**) (0.15-0.30 g; 0.87-1.75 mmol) was dissolved in absolute ethanol (12.0 mL). Next, the corresponding aldehyde (0.12-0.29 g; 0.97-1.85 mmol) and three drops of hydrochloric acid 37 % were added and the reaction mixture was stirred at room temperature for 0.5-3.5 hours, until TLC examination indicated the end of reaction. Isolation was performed by product precipitation after adding crushed ice to the flask. Products **8a-t** were collected by vacuum filtration and purified properly by recrystallization from absolute ethanol if necessary.

(E)-3-amino-N'-(benzylidene)-4-methylthiophene-2-carbohydrazide (8a; LASSBio 1881)

Obtained after 0.5 hour of reaction between the key intermediate **10** (0.25 g; 1.46 mmol) and benzaldehyde (0.17 g; 0.16 mL; 1.56 mmol) as a yellow crystalline solid. Yield 88.9%; m.p. 202 °C; MS (EI) m/z calcd for $\text{C}_{13}\text{H}_{13}\text{N}_3\text{OS}$ (M+) 259; found 260 (MH+); HPLC (A, 342 nm) = 99.2 %.

IR (ATR) ν_{max} (cm^{-1}): 3401 ($\nu_{\text{as}}\text{NH}_2$); 3303 ($\nu_{\text{s}}\text{NH}_2$); 3137 (νNH); 3025 (νCH); 2925 (νCH_3); 1622 ($\nu\text{C}=\text{O}$); 1591 ($\nu\text{C}=\text{N}$); 1555 (δNH); 1440 (νCC); 1369 (νNH).

^1H NMR (200 MHz, DMSO-*d*6) δ (ppm) (Supplementary Material - Figure S1): 2.04 (s, 3H, CH_3); 6.86 (s, 2H, NH_2); 7.31 (s, 1H, H5); 7.35-7.55 (m, 3H, H3' & H4' & H5'); 7.76 (d, 2H, $J=7.17$ Hz, H2' & H6'); 8.02 (s, 1H, N=CH); 11.2 (s, 1H, CONH).

^{13}C NMR (50 MHz, DMSO-*d*6) δ (ppm) (Figure S2): 12.8 (CH_3); 97.0 (C2); 127 (C2' &

C6'); 129 (C3' & C4' & C5'); 129 (C4); 130 (C1'); 135 (C5); 142 (C3); 156 (N=CH); 165 (CONH).

(E)-3-amino-N'-(4-bromobenzylidene)-4-methylthiophene-2-carbohydrazide (8b; LASSBio 1879)

Obtained after 2 hours of reaction between the key intermediate **10** (0.20 g; 1.16 mmol) and 4-bromobenzaldehyde (0.24 g; 1.26 mmol) as a yellow crystalline solid. Yield 93.0%; m.p. 250 °C; MS (EI) m/z calcd for $\text{C}_{13}\text{H}_{12}\text{BrN}_3\text{OS}$ (M+) 337 and 339; found 338 and 340 (MH+); HPLC (B, 342 nm) = 99.4%.

IR (ATR) ν_{max} (cm^{-1}): 3393 ($\nu_{\text{as}}\text{NH}_2$); 3293 ($\nu_{\text{s}}\text{NH}_2$); 3137 (νNH); 2918 (νCH_3); 1622 ($\nu\text{C}=\text{O}$); 1591 ($\nu\text{C}=\text{N}$); 1556 (δNH); 1440 (νCC); 1373 (νNH); 1061 (νCBr).

^1H NMR (200 MHz, DMSO-*d*6) δ (ppm): 2.04 (s, 3H, CH_3); 6.87 (s, 2H, NH_2); 7.30 (s, 1H, H5); 7.50-7.84 (m, 4H, H2' & H3' & H5' & H6'); 7.99 (s, 1H, N=CH); 11.3 (s, 1H, CONH).

^{13}C NMR (50 MHz, DMSO-*d*6) δ (ppm): 12.8 (CH_3); 96.8 (C2); 123 (C4'); 127 (C4); 129 (C2' & C4'); 130 (C1'); 132 (C3' & C5'); 134 (C5); 141 (C3); 156 (N=CH); 165 (CONH).

(E)-3-amino-4-methyl-N'-(4-nitrobenzylidene)thiophene-2-carbohydrazide (8c; LASSBio 1890)

Obtained after 1.5 hours of reaction between the key intermediate **10** (0.25 g; 1.46 mmol) and 4-nitrobenzaldehyde (0.24 g; 1.56 mmol) as an orange crystalline solid. Yield 93.5%; m.p. 297 °C; MS (EI) m/z calcd for $\text{C}_{13}\text{H}_{12}\text{N}_4\text{O}_3\text{S}$ (M+) 304; found 305 (MH+); HPLC (A, 364 nm) = 99.0 %.

IR (ATR) ν_{max} (cm^{-1}): 3484 ($\nu_{\text{as}}\text{NH}_2$); 3367 ($\nu_{\text{s}}\text{NH}_2$); 3146 (νNH); 3034 (νCH); 2931 (νCH_3); 1623 ($\nu\text{C}=\text{O}$); 1592 ($\nu\text{C}=\text{N}$); 1548 (δNH); 1510 ($\nu_{\text{as}}\text{NO}_2$); 1449 (νCC); 1381 (νNH); 1328 ($\nu_{\text{s}}\text{NO}_2$).

^1H NMR (200 MHz, DMSO-*d*6) δ (ppm): 2.04 (s, 3H, CH_3); 6.93 (s, 2H, NH_2); 7.33 (s, 1H, H5); 7.99 (d, 2H, $J=8.73$ Hz, H2' & H6'); 8.11 (s,

1H, N=CH); 8.30 (d, 2H, J=8.78 Hz, H3' & H5'); 11.5 (s, 1H, CONH).

¹³C NMR (50 MHz, DMSO-*d*6) δ (ppm): 12.8 (CH₃); 96.5 (C2); 124 (C3' & C5'); 127 (C4); 128 (C2' & C4'); 130 (C1'); 139 (C4'); 141 (C5); 147 (C3); 156 (N=CH); 165 (CONH).

(E)-3-amino-*N'*-(4-hydroxybenzylidene)-4-methylthiophene-2-carbohydrazide (**8d**; LASSBio 1895)

Obtained after 2 hours of reaction between the key intermediate **10** (0.15 g; 0.87 mmol) and 4-hydroxybenzaldehyde (0.12 g; 0.97 mmol) as a yellow crystalline solid. Yield 63.7%; m.p. 233 °C; MS (EI) *m/z* calcd for C₁₃H₁₃N₃O₂S (M⁺) 275; found 276 (MH⁺); HPLC (A, 342 nm) = 99.6 %.

IR (ATR) v_{max} (cm⁻¹): 3363 (νNH₂); 3058 (νNH); 2941 (νCH₃); 1628 (νC=O); 1610 (νC=N); 1584 (δNH); 1445 (νCC); 1393 (νNH); 1228 (δOH).

¹H NMR (200 MHz, DMSO-*d*6) δ (ppm): 2.05 (s, 3H, CH₃); 7.33 (s, 1H, H5); 7.99 (d, 2H, J=8.53 Hz, H2' & H6'); 8.12 (s, 1H, N=CH); 8.30 (d, 2H, J=8.51 Hz, H3' & H5'); 11.5 (s, 1H, CONH).

¹³C NMR (50 MHz, DMSO-*d*6) δ (ppm): 12.9 (CH₃); 102 (C2); 116 (C3' & C5'); 126 (C1'); 128 (C4); 129 (C2' & C4'); 132 (C5); 143 (C3); 152 (N=CH); 159 (C4'); 164 (CONH).

(E)-4-((2-(3-amino-4-methylthiophene-2-carbonyl)hydrazono)methyl)benzoic acid (**8e**; LASSBio 1873)

Obtained after 1 hour of reaction between the key intermediate **10** (0.30 g; 1.75 mmol) and 4-formylbenzoic acid (0.29 g; 1.85 mmol) as a yellow crystalline solid. Yield 89.5%; m.p. 140 °C; MS (EI) *m/z* calcd for C₁₄H₁₃N₃O₃S (M⁺) 303; found 304 (MH⁺); HPLC (A, 342 nm) = 99.7 %.

IR (ATR) v_{max} (cm⁻¹): 3374 (νNH₂); 3231 (νNH); 2926 (νCH₃); 1698 (νC=O & νCOOH); 1590 (νC=O); 1442 (νCC); 1384 (νNH).

¹H NMR (200 MHz, DMSO-*d*6) δ (ppm): 2.04 (s, 3H, CH₃); 7.32 (s, 1H, H5); 7.86 (d, 2H, J=7.87 Hz, H2' & H6'); 8.01 (d, 2H, J=7.91 Hz, H3' & H5'); 8.08 (s, 1H, N=CH); 11.4 (s, 1H, CONH); 13.0 (s, 1H, COOH).

¹³C NMR (50 MHz, DMSO-*d*6) δ (ppm): 12.9 (CH₃); 96.9 (C2); 127 (C2' & C6'); 127 (C4); 130 (C3' & C5'); 130 (C1'); 131 (C4'); 139 (C5); 141 (C3); 156 (N=CH); 165 (CONH); 167 (COOH).

(E)-3-amino-*N'*-(4-(dimethylamino)benzylidene)-4-methylthiophene-2-carbohydrazide (**8f**; LASSBio 1888)

Obtained after 2 hours of reaction between the key intermediate **10** (0.20 g; 1.16 mmol) and 4-(dimethylamino)benzaldehyde (0.19 g; 1.26 mmol) as an orange crystalline solid. Yield 44.6%; m.p. 164 °C; MS (EI) *m/z* calcd for C₁₅H₁₈N₄OS (M⁺) 302; found 303 (MH⁺); HPLC (A, 364 nm) = 97.7 %.

IR (ATR) v_{max} (cm⁻¹): 3410 (ν_{as}NH₂); 3346 (ν_sNH₂); 3299 (νNH); 2913 (νCH₃); 1593 (νC=O); 1443 (νCC); 1361 (νNH); 1185 (νCN).

¹H NMR (200 MHz, DMSO-*d*6) δ (ppm) (Figure S3): 2.05 (s, 3H, CH₃); 3.00 (s, 6H, N(CH₃)₂); 7.05 (d, 2H, J=7.94 Hz; H3' & H5'); 7.31 (s, 1H, H5); 7.66 (d, 2H, J=8.33 Hz, H2' & H6'); 7.95 (s, 1H, N=CH); 11.1 (s, 1H, CONH).

¹³C NMR (50 MHz, DMSO-*d*6) δ (ppm) (Figure S4): 12.9 (CH₃); 41.1 (N(CH₃)₂); 98.8 (C2); 114 (C3' & C5'); 125 (C1'); 127 (C4); 128 (C2' & C6'); 130 (C4); 142 (C3); 149 (C4'); 154 (N=CH); 165 (CONH).

(E)-3-amino-*N'*-(4-methoxybenzylidene)-4-methylthiophene-2-carbohydrazide (**8g**; LASSBio 1874)

Obtained after 2 hours of reaction between the key intermediate **10** (0.20 g; 1.16 mmol) and 4-methoxybenzaldehyde (0.17 g; 0.16 mL; 1.26 mmol) as a yellow crystalline solid. Yield 76.0%; m.p. 176 °C; MS (EI) *m/z* calcd for C₁₄H₁₅N₃O₂S (M⁺) 289; found 290 (MH⁺); HPLC (A, 342 nm) = 99.6 %.

IR (ATR) ν_{\max} (cm⁻¹): 3464 (vasNH₂); 3397 (vsNH₂); 3302 (vNH); 3136 (vCH); 2926 (vCH₃); 1608 (vC=O); 1591 (vC=N); 1555 (δ NH); 1441 (vCC); 1386 (vNH); 1249 (vCOC).

¹H NMR (200 MHz, DMSO-*d*6) δ (ppm): 2.03 (s, 3H, CH₃); 3.79 (s, 3H, OCH₃); 6.83 (s, 2H, NH₂); 7.02 (d, 2H, J=8.29 Hz, H_{3'} & H_{5'}); 7.29 (s, 1H, H₅); 7.70 (d, 2H, J=8.16 Hz, H_{2'} & H_{6'}); 7.96 (s, 1H, N=CH); 11.1 (s, 1H, CONH).

¹³C NMR (50 MHz, DMSO-*d*6) δ (ppm): 12.9 (CH₃); 55.3 (OCH₃); 102 (C₂); 114 (C_{3'} & C_{5'}); 127 (C_{1'}); 128 (C₄); 129 (C_{2'} & C_{4'}); 130 (C₅); 143 (C₃); 151 (N=CH); 161 (C_{4'}); 164 (CONH).

(E)-3-amino-*N'*-(4-isopropylbenzylidene)-4-methylthiophene-2-carbohydrazide (**8h**; LASSBio 1892)

Obtained after 0.5 hour of reaction between the key intermediate **10** (0.25 g; 1.46 mmol) and 4-isopropylbenzaldehyde (0.24 g; 0.24 mL; 1.56 mmol) as a yellow crystalline solid. Yield 81.5%; m.p. 169 °C; MS (EI) *m/z* calcd for C₁₆H₁₉N₃O₂S (M⁺) 301; found 302 (MH⁺); HPLC (B, 342 nm) = 99.2 %.

IR (ATR) ν_{\max} (cm⁻¹): 3451 (v_{as}NH₂); 3332 (v_sNH₂); 2958 (vCH₃); 1634 (vC=O); 1600 (vC=N); 1551 (δ NH); 1449 (vCC); 1381 (vNH).

¹H NMR (200 MHz, DMSO-*d*6) δ (ppm) (Figure S5): 1.21 (d, 6H, J=6.77 Hz, CH(CH₃)₂); 2.06 (s, 3H, CH₃); 2.90 (m, 1H, J=6.77 Hz, CH(CH₃)₂); 7.25-7.40 (m, 3H, H₅ & H_{3'} & H_{5'});

7.68 (d, 2H, J=7.87 Hz, H_{2'} & H_{6'}); 8.02 (s, 1H, N=CH); 11.23 (s, 1H, CONH).

¹³C NMR (50 MHz, DMSO-*d*6) δ (ppm) (Figure S6): 12.9 (CH₃); 23.6 (CH(CH₃)₂); 33.3 (CH(CH₃)₂); 98.4 (C₂); 127 (C_{3'} & C_{5'}); 127 (C_{2'} & C_{6'}); 127 (C_{1'}); 130 (C₄); 132 (C₅); 142 (C₃); 150 (N=CH); 155 (C_{4'}); 165 (CONH).

(E)-3-amino-4-methyl-*N'*-(4-phenoxybenzylidene)thiophene-2-carbohydrazide (**8i**; LASSBio 1887)

Obtained after 2 hours of reaction between the key intermediate **10** (0.20 g; 1.16 mmol) and 4-phenoxybenzaldehyde (0.25 g; 0.22 mL; 1.26 mmol) as a yellow crystalline solid. Yield 92.1%; m.p. 207 °C; MS (EI) *m/z* calcd for C₁₉H₁₇N₃O₂S (M⁺) 351; found 352 (MH⁺); HPLC (B, 342 nm) = 99.8 %.

IR (ATR) ν_{\max} (cm⁻¹): 3454 (vasNH₂); 3332 (vsNH₂); 3139 (vNH); 2924 (vCH₃); 1633 (vC=O); 1585 (vC=N); 1552 (δ NH); 1445 (vCC); 1382 (vNH); 1242 (vCOC).

¹H NMR (200 MHz, DMSO-*d*6) δ (ppm) (Figure S7): 2.03 (s, 3H, CH₃); 6.80 (s, 2H, NH₂); 7.07 (m, 4H, H_{3'} & H_{5'} & H_{2''} & H_{6''}); 7.19 (t, 1H, J=7.43 Hz, H_{4''}); 7.27 (s, 1H, H₅); 7.42 (t, 2H, J=8.27 Hz, H_{3''} & H_{5''}); 7.77 (d, 2H, J=8.55 Hz, H_{2'} & H_{6'}); 8.01 (s, 1H, N=CH); 11.12 (s, 1H, CONH).

¹³C NMR (50 MHz, DMSO-*d*6) δ (ppm) (Figure S8): 13.0 (CH₃); 97.2 (C₂); 119 (C_{2''} & C_{4''}); 119 (C_{3'} & C_{5'}); 124 (C_{4''}); 127 (C₄ & C_{1'}); 129 (C_{2'} & C_{6'}); 130 (C₅); 130 (C_{3''} & C_{5''}); 142 (C₃); 156 (N=CH); 156 (C_{4'}); 158 (C_{1''}); 165 (CONH).

(E)-3-amino-*N'*-(biphenyl-4-ylmethylene)-4-methylthiophene-2-carbohydrazide (**8j**; LASSBio 1875)

Obtained after 3 hours of reaction between the key intermediate **10** (0.20 g; 1.16 mmol) and biphenyl-4-carbaldehyde (0.23 g; 1.26 mmol) as a yellow

crystalline solid. Yield 95.1%; m.p. 217 °C; MS (EI) m/z calcd for C₁₉H₁₇N₃OS (M⁺) 335; found 336 (MH⁺); HPLC (B, 342 nm) = 99.8 %.

IR (ATR) ν_{\max} (cm⁻¹): 3351 (vasNH₂); 2832 (vCH); 1622 (vC=O); 1552 (vsNO₂); 1484 (vCC); 1346 (vasNO₂); 1372 (vNH).

¹H NMR (200 MHz, DMSO-*d*₆) δ (ppm) (Figure S9): 2.05 (s, 3H, CH₃); 7.30-7.55 (m, 4H, H₅ & H_{3''} & H_{4''} & H_{5''}); 7.65-7.95 (m, 6H; H_{2'} & H_{3'} & H_{5'} & H_{6'} & H_{2''} & H_{6''}); 8.07 (s, 1H, N=CH); 11.3 (s, 1H, CONH).

¹³C NMR (50 MHz, DMSO-*d*₆) δ (ppm) (Figure S10): 13.0 (CH₃); 97.1 (C₂); 127 (C_{2''} & C_{6''}); 127 (C_{3'} & C_{5'} & C_{4''}); 128 (C_{2'} & C_{6'}); 128 (C₄); 129 (C_{3''} & C_{5''}); 130 (C_{1'}); 134 (C₅); 139 (C_{1''}); 141 (C_{4'}); 142 (C₃); 156 (N=CH); 165 (CONH).

(E)-3-amino-4-methyl-*N'*-(naphthalen-1-ylmethylene)thiophene-2-carbohydrazide (**8k**); LASSBio 1877)

Obtained after 3.5 hours of reaction between the key intermediate **10** (0.20 g; 1.16 mmol) and 1-naphthaldehyde (0.20 g; 1.26 mmol) as a yellow crystalline solid. Yield 89.5%; m.p. 247 °C; MS (EI) m/z calcd for C₁₇H₁₅N₃OS (M⁺) 309; found 310 (MH⁺); HPLC (B, 342 nm) = 98.9 %.

IR (ATR) ν_{\max} (cm⁻¹): 3472 (vasNH₂); 3349 (vsNH₂); 2923 (vCH₃); 1622 (vC=O); 1602 (vC=N); 1546 (δ NH); 1460 (vCC); 1389 (vNH).

¹H NMR (200 MHz, DMSO-*d*₆) δ (ppm) (Figure S11): 2.06 (s, 3H, CH₃); 6.89 (s, 2H, NH₂); 7.35 (s, 1H, H₅); 7.50-7.60 (m, 2H, H_{2'} & H_{3'}); 7.85-7.03 (m, 3H, H_{4'} & H_{6'} & H_{7'}); 8.07 (s, 1H, N=CH); 8.09-8.25 (m, 2H, H_{5'} & H_{8'}); 11.3 (s, 1H, CONH).

¹³C NMR (50 MHz, DMSO-*d*₆) δ (ppm) (Figure S12): 12.9 (CH₃); 97.0 (C₂); 123 (C_{8'}); 127 (C_{2''}); 127 (C_{3''}); 127 (C_{6''}); 128 (C_{7''}); 128 (C_{4'}); 128 (C_{5'}); 128 (C_{8'a}); 130 (C_{4'a}); 132

(C₄); 133 (C_{1'}); 133 (C₅); 142 (C₃); 156 (N=CH); 165 (CONH).

(E)-3-amino-4-methyl-*N'*-(naphthalen-2-ylmethylene)thiophene-2-carbohydrazide (**8l**); LASSBio 1889)

Obtained after 1.5 hours of reaction between the key intermediate **10** (0.20 g; 1.16 mmol) and 2-naphthaldehyde (0.20 g; 1.26 mmol) as a yellow crystalline solid. Yield 95.5%; m.p. 248 °C; MS (EI) m/z calcd for C₁₇H₁₅N₃OS (M⁺) 309; found 310 (MH⁺); HPLC (B, 342 nm) = 98.9 %.

IR (ATR) ν_{\max} (cm⁻¹): 3472 (vasNH₂); 3349 (vsNH₂); 2923 (vCH₃); 1622 (vC=O); 1602 (vC=N); 1546 (δ NH); 1460 (vCC); 1389 (vNH).

¹H NMR (200 MHz, DMSO-*d*₆) δ (ppm): 2.06 (s, 3H, CH₃); 6.89 (s, 2H, NH₂); 7.35 (s, 1H, H₅); 7.48-7.65 (m, 2H, H_{3'} & H_{6'}); 7.85-8.03 (m, 3H, H_{1'} & H_{7'} & H_{8'}); 8.07 (s, 1H, N=CH); 8.12 (d, 1H, J=8.31 Hz, H_{4'}); 8.20 (m, 1H, H_{5'}); 11.3 (s, 1H, CONH).

¹³C NMR (50 MHz, DMSO-*d*₆) δ (ppm): 12.9 (CH₃); 97.0 (C₂); 123 (C_{3''}); 127 (C_{1''}); 127 (C_{6''}); 127 (C_{7''}); 128 (C_{5''}); 128 (C_{8''}); 128 (C_{4''}); 129 (C_{4'a}); 130 (C_{8'a}); 132 (C₄); 133 (C_{2'}); 133 (C₅); 142 (C₃); 156 (N=CH); 165 (CONH).

(E)-2-((2-(3-amino-4-methylthiophene-2-carbonyl)hydrazon)methyl) ferrocene (**8m**); LASSBio 1876)

Obtained after 0.5 hour of reaction between the key intermediate **10** (0.30 g; 1.75 mmol) and ferrocenecarbaldehyde (0.41 g; 1.85 mmol) as a brown crystalline solid. Yield 93.1%; m.p. 57 °C; MS (EI) m/z calcd for C₁₇H₁₇FeN₃OS (M⁺) 367; found 368 (MH⁺); HPLC (A, 332 nm) = 99.2 %.

IR (ATR) ν_{\max} (cm⁻¹): 3427 (vasNH₂); 3312 (vsNH₂); 3087 (vCH); 2919 (vCH₃); 1620 (vC=O); 1588 (vC=N); 1547 (δ NH); 1438 (vCC); 1384 (vNH).

¹H NMR (200 MHz, DMSO-*d*6) δ (ppm): 2.03 (s, 3H, CH₃); 4.19 (s, 5H, H1'' & H2'' & H3'' & H4'' & H5''); 4.40 (s, 2H, H3' & H4'); 4.69 (s, 2H, H2' & H5'); 6.78 (s, 2H, NH₂); 7.26 (s, 1H, H5); 7.81 (s, 1H, N=CH); 11.0 (s, 1H, CONH).

¹³C NMR (50 MHz, DMSO-*d*6) δ (ppm): 12.8 (CH₃); 67.4 (C3' & C4'); 68.9 (C1'' & C2'' & C3'' & C4'' & C5''); 69.7 (C2' & C3'); 79.53 (C1'); 97.7 (C2); 127 (C4); 130 (C5); 142 (C3); 155 (N=CH); 164 (CONH).

(E)-3-amino-*N'*-(furan-2-ylmethylene)-4-methylthiophene-2-carbohydrazide (**8n**; LASSBio 1872)

Obtained after 0.5 hour of reaction between the key intermediate **10** (0.30 g; 1.75 mmol) and furan-2-carbaldehyde (0.19 g; 0.16 mL; 1.85 mmol) as a brown crystalline solid. Yield 77.3%; m.p. 178 °C; MS (EI) *m/z* calcd for C₁₁H₁₁N₃O₂S (M⁺) 249; found 250 (MH⁺); HPLC (A, 300 nm) = 99.6 %.

IR (ATR) ν_{\max} (cm⁻¹): 3464 (vasNH₂); 3327 (vsNH₂); 3136 (vNH); 2916 (vCH₃); 1617 (vC=O); 1588 (vC=N); 1547 (δNH); 1442 (vCC); 1372 (vNH).

¹H NMR (200 MHz, DMSO-*d*6) δ (ppm): 2.02 (s, 3H, CH₃); 6.50-6.95 (m, 4H, NH₂ & H3' & H4'); 7.26 (s, 1H, H5); 7.83 (m, 1H, H5'); 7.94 (s, 1H, N=CH); 11.1 (s, 1H, CONH).

¹³C NMR (50 MHz, DMSO-*d*6) δ (ppm): 13.2 (CH₃); 97.4 (C2); 112 (C3'); 112 (C4'); 127 (C2'); 130 (C4); 132 (C5); 145 (C3); 150 (C5'); 156 (N=CH); 165 (CONH).

(E)-3-amino-*N'*-(furan-3-ylmethylene)-4-methylthiophene-2-carbohydrazide (**8o**; LASSBio 1880)

Obtained after 3 hours of reaction between the key intermediate **10** (0.21 g; 1.22 mmol) and furan-3-carbaldehyde (0.17 g; 0.15 mL; 1.32 mmol) as a yellow crystalline solid. Yield 58.9%; m.p. 179

°C; MS (EI) *m/z* calcd for C₁₁H₁₁N₃O₂S (M⁺) 249; found 250 (MH⁺); HPLC (A, 332 nm) = 99.2 %.

IR (ATR) ν_{\max} (cm⁻¹): 3471 (vasNH₂); 3349 (vsNH₂); 3126 (vNH); 2927 (vCH₃); 1629 (vC=O); 1590 (vC=N); 1550 (δNH); 1441 (vCC); 1373 (vNH).

¹H NMR (200 MHz, DMSO-*d*6) δ (ppm) (Figure S13): 2.03 (s, 3H, CH₃); 6.87 (m, 1H, H4'); 7.26 (s, 1H, H5); 7.70-7.80 (m, 1H, H5'); 7.98 (s, 1H, N=CH); 8.06-8.10 (m, 1H, H2'); 11.2 (s, 1H, CONH).

¹³C NMR (50 MHz, DMSO-*d*6) δ (ppm) (Figure S14): 12.9 (CH₃); 98.0 (C2); 108 (C4'); 123 (C3'); 127 (C5'); 130 (C2'); 134 (C4); 144 (C5); 145 (C3); 155 (N=CH); 165 (CONH).

(E)-*N'*-((1*H*-pyrrol-2-yl)methylene)-3-amino-4-methylthiophene-2-carbohydrazide (**8p**; LASSBio 1894)

Obtained after 3.5 hours of reaction between the key intermediate **10** (0.25 g; 1.46 mmol) and 1*H*-pyrrole-2-carbaldehyde (0.15 g; 1.56 mmol) as a violet crystalline solid. Yield 42.4%; m.p. 82.2 °C; MS (EI) *m/z* calcd for C₁₁H₁₂N₄OS (M⁺) 248; found 249 (MH⁺); HPLC (B, 342 nm) = 99.2 %.

IR (ATR) ν_{\max} (cm⁻¹): 3207 (vNH); 1644 (vC=O); 1592 (vC=N); 1548 (δNH); 1470 (vCC); 1304 (vNH).

¹H NMR (200 MHz, DMSO-*d*6) δ (ppm): 2.02 (s, 3H, CH₃); 6.10-6.20 (m, 1H, H4'); 6.45-6.55 (m, 1H, H3'); 6.87-6.95 (m, 1H, H5'); 7.22 (s, 1H, H5); 7.92 (s, 1H, N=CH); 10.8-11.1 (m, 2H, H1' & CONH).

¹³C NMR (50 MHz, DMSO-*d*6) δ (ppm): 12.9 (CH₃); 98.2 (C2); 109 (C4'); 122 (C3'); 127 (C5'); 128 (C2'); 129 (C4); 135 (C5); 141 (C3); 156 (N=CH); 164 (CONH).

(E)-3-amino-4-methyl-*N'*-(thiophen-2-ylmethylene)thiophene-2-carbohydrazide (**8g**;
LASSBio 1886)

Obtained after 3.5 hours of reaction between the key intermediate **10** (0.28 g; 1.63 mmol) and thiophene-2-carbaldehyde (0.20 g; 0.17 mL; 1.73 mmol) as a brown crystalline solid. Yield 86.4%; m.p. 209 °C; MS (EI) m/z calcd for C₁₁H₁₁N₃OS₂ (M⁺) 265; found 266 (MH⁺); HPLC (A, 332 nm) = 99.5 %.

IR (ATR) v_{max} (cm⁻¹): 3465 (vasNH₂); 3331 (vsNH₂); 3129 (vNH); 2922 (vCH₃); 1617 (vC=O); 1582 (vC=N); 1541 (δNH); 1444 (vCC); 1385 (vNH).

¹H NMR (200 MHz, DMSO-*d*6) δ (ppm): 2.03 (s, 3H, CH₃); 6.81 (s, 2H, NH₂); 7.10 (t, 1H, J=3.92 Hz, H₄'); 7.29 (s, 1H, H₅); 7.39 (d, 1H, J=2.42 Hz, H₃'); 7.61 (d, 1H, J=4.63 Hz, H₅'); 8.21 (s, 1H, N=CH); 11.2 (s, 1H, CONH).

¹³C NMR (50 MHz, DMSO-*d*6) δ (ppm): 12.9 (CH₃); 97.3 (C₂); 127 (C₄'); 128 (C₅'); 128 (C₃'); 130 (C₄ & C₂'); 137 (C₅); 139 (C₃); 156 (N=CH); 165 (CONH).

(E)-3-amino-4-methyl-*N'*-(thiophen-3-ylmethylene)thiophene-2-carbohydrazide (**8r**;
LASSBio 1878)

Obtained after 3.5 hours of reaction between the key intermediate **10** (0.20 g; 1.16 mmol) and thiophene-3-carbaldehyde (0.14 g; 0.11 mL; 1.26 mmol) as a dark yellow crystalline solid. Yield 75.1%; m.p. 187 °C; MS (EI) m/z calcd for C₁₁H₁₁N₃OS₂ (M⁺) 265; found 266 (MH⁺); HPLC (A, 332 nm) = 99.0 %.

IR (ATR) v_{max} (cm⁻¹): 3457 (vasNH₂); 3330 (vsNH₂); 3132 (vNH); 2922 (vCH₃); 1621 (vC=O); 1586 (vC=N); 1542 (δNH); 1446 (vCC); 1380 (vNH).

¹H NMR (200 MHz, DMSO-*d*6) δ (ppm): 2.03 (s, 3H, CH₃); 6.83 (s, 2H, NH₂); 7.28 (s, 1H,

H₅); 7.56-7.68 (m, 2H, H₄' & H₅'); 7.82-7.88 (m, 1H, H₂'); 8.05 (s, 1H, N=CH); 11.1 (s, 1H, CONH).

¹³C NMR (50 MHz, DMSO-*d*6) δ (ppm): 12.9 (CH₃); 97.2 (C₂); 125 (C₄'); 127 (C₅'); 127 (C₂'); 127 (C₃'); 130 (C₄); 137 (C₅); 138 (C₃); 156 (N=CH); 165 (CONH).

(E)-3-amino-4-methyl-*N'*-(pyridin-3-ylmethylene)thiophene-2-carbohydrazide (**8s**;
LASSBio 1891)

Obtained after 0.5 hour of reaction between the key intermediate **10** (0.25 g; 1.46 mmol) and nicotinaldehyde (0.17 g; 0.15 mL; 1.56 mmol) as a yellow crystalline solid. Yield 52.4%; m.p. 266 °C (degradation); MS (EI) m/z calcd for C₁₂H₁₂N₄OS (M⁺) 260; found 261 (MH⁺); HPLC (A, 342 nm) = 99.0 %.

IR (ATR) v_{max} (cm⁻¹): 3429 (vasNH₂); 3327 (vsNH₂); 3064 (vNH); 3012 (vCH); 2923 (vCH₃); 1607 (vC=O); 1574 (vC=N); 1538 (δNH); 1444 (vCC); 1378 (vNH).

¹H NMR (200 MHz, DMSO-*d*6) δ (ppm): 2.04 (s, 3H, CH₃); 7.34 (s, 1H, H₅); 7.86 (t, 1H, J=6.74 Hz, H₅'); 8.12 (s, 1H, N=CH); 8.56 (d, 1H, J=7.80 Hz, H₄'); 8.76 (d, 1H, J=4.50 Hz; H₆'); 9.04 (s, 1H, H₂'); 11.6 (s, 1H, CONH).

¹³C NMR (50 MHz, DMSO-*d*6) δ (ppm): 12.9 (CH₃); 96.6 (C₂); 126 (C₅'); 127 (C₄); 130 (C₅); 133 (C₃'); 137 (C₃); 139 (C₄'); 143 (C₂'); 144 (C₆'); 156 (N=CH); 165 (CONH).

(E)-3-amino-4-methyl-*N'*-(pyridin-4-ylmethylene)thiophene-2-carbohydrazide (**8t**;
LASSBio 1893)

Obtained after 0.5 hour of reaction between the key intermediate **10** (0.30 g; 1.75 mmol) and isonicotinaldehyde (0.21 g; 0.18 mL; 1.85 mmol) as a yellow crystalline solid. yield 93.1%; m.p. 286 °C (degradation); MS (EI) m/z calcd for C₁₂H₁₂N₄OS (M⁺) 260; found 261 (MH⁺); HPLC (A, 342 nm) = 99.4 %.

IR (ATR) ν_{\max} (cm⁻¹): 3416 (vasNH₂); 3307 (vsNH₂); 3084 (vNH); 1598 (vC=O); 1572 (vC=N); 1548 (δ NH); 1446 (vCC); 1356 (vNH).

¹H NMR (200 MHz, DMSO-*d*₆) δ (ppm): 2.05 (s, 3H, CH₃); 7.38 (s, 1H, H₅); 8.16 (s, 1H, N=CH); 8.21 (d, 2H, J=6.69 Hz, H_{3'} & H_{5'}); 8.89 (d, 2H, J=6.65 Hz, H_{2'} & H_{6'}); 12.0 (s, 1H, CONH).

¹³C NMR (50 MHz, DMSO-*d*₆) δ (ppm): 12.9 (CH₃); 95.9 (C₂); 123 (C_{3'} & C_{5'}); 127 (C₄); 131 (C₅); 137 (C₃); 143 (C_{2'} & C_{6'}); 149 (C_{4'}); 157 (N=CH); 165 (CONH).

ACKNOWLEDGMENTS

The authors would like to thank the Conselho Nacional de Desenvolvimento Científico e Tecnológico (CNPq - BR), the Baden-Württemberg Stiftung (DE), the Fundação Carlos Chagas Filho de Amparo à Pesquisa do Estado do Rio de Janeiro (FAPERJ - BR) and Instituto Nacional de Ciência e Tecnologia de Fármacos e Medicamentos (INCT-INOVAR - BR, Grant CNPq 573.564/2008-6 and FAPERJ E-26/170.020/2008) for fellowship and financial support.

REFERENCES

- ABDEL-AZIZ HA, ABOUL-FADL T, AL-OBAID ARM, GHAZZALI M, AL-DHFYAN A AND CONTINI A. 2012. Design, synthesis and pharmacophoric model building of novel substituted nicotinic acid hydrazones with potential antiproliferative activity. *Arch Pharm Res* 35: 1543-1552.
- AL-NURI MA AND HUSEIN AI. 2011. Synthesis and Biological Activity of N-Heteroaromatic Substituted Thiophene-2- Carbohydrazides. *J Chem Chem Eng* 5: 648-651.
- ANAND P, SHENOY R, PALMER JE, BAINES AJ, LAI RYK, ROBERTSON J, BIRD N, OSTENFELD T AND CHIZH BA. 2011. Clinical trial of the p38 MAP kinase inhibitor dilmapiomod in neuropathic pain following nerve injury. *Eur J Pain* 15: 1040-1048.
- AZIZIAN H, MOUSAVI Z, FARAJI H, TAJIK M, BAGHERZADEH K, BAYAT P, SHAFIEE A AND ALMASIRAD A. 2016. Arylhydrazone derivatives of naproxen as new analgesic and anti-inflammatory agents: Design, synthesis and molecular docking studies. *J Mol Graph Model* 67: 127-136.
- BARREIRO EJ, KÜMMERLE AE AND FRAGA CAM. 2011. The methylation effect in medicinal chemistry. *Chem Rev* 111: 5215-5246.
- COELHO AA, EVANS J, EVANS I, KERN A AND PARSONS S. 2011. The TOPAS symbolic computation system. *Powder Diffr* 26: S22-S25.
- COLLIER HO, DINNEEN LC, JOHNSON CA AND SCHNEIDER C. 1968. The abdominal constriction response and its suppression by analgesic drugs in the mouse. *Br J Pharmacol Chemother* 32: 295-310.
- COSTA FN, DA SILVA TF, SILVA EMB, BARROSO RCR, BRAZ D, BARREIRO EJ, LIMA LM, PUNZO F AND FERREIRA FF. 2015. Structural feature evolution – from fluids to the solid phase – and crystal morphology study of LASSBio 1601: a cyclohexyl-N-acylhydrazone derivative. *RSC Adv* 5: 39889-39898.
- COSTA FN, FERREIRA FF, DA SILVA TF, BARREIRO EJ, LIMA LM, BRAZ D AND BARROSO RC. 2013. Structure re-determination of LASSBio-294 - a cardioactive compound of the N-acylhydrazone class - using X-ray powder diffraction data. *Powder Diffr* 28: S491-S509.
- CUTSHALL NS ET AL. 2012. Novel 2-methoxyacylhydrazones as potent, selective PDE10A inhibitors with activity in animal models of schizophrenia. *Bioorg Med Chem Lett* 22: 5595-5599.
- DA SILVA YKC, REYES CTM, RIVERA G, ALVES MA, BARREIRO EJ, MOREIRA MSA AND LIMA LM. 2014. 3-Aminothiophene-2-acylhydrazones: Non-toxic, analgesic and anti-inflammatory lead-candidates. *Molecules* 19: 8456-8471.
- DAVID WIF, SHANKLAND K, VAN DE STREEK J, PIDCOCK E, MOTHERWELL WDS AND COLE JC. 2006. DASH: A program for crystal structure determination from powder diffraction data. *J Appl Crystallogr* 39: 910-915.
- DE FIGUEIREDO LP, IBIAPINO AL, DO AMARAL DN, FERRAZ LS, RODRIGUES T, BARREIRO EJ, LIMA LM AND FERREIRA FF. 2017. Structural characterization and cytotoxicity studies of different forms of a combretastatin A4 analogue. *J Mol Struct* 1147: 226-234.
- DUARTE CD, BARREIRO EJ AND FRAGA CAM. 2007. Privileged structures: a useful concept for the rational design of new lead drug candidates. *Mini Rev Med Chem* 7: 1108-1119.
- EVANS BE ET AL. 1988. Methods for drug discovery: development of potent, selective, orally effective cholecystokinin antagonists. *J Med Chem* 31: 2235-2246.
- GAGE JL ET AL. 2011. N-Acylhydrazones as inhibitors of PDE10A. *Bioorg Med Chem Lett* 21: 4155-4159.

- GOETTERT M, GRAESER R AND LAUFER SA. 2010. Optimization of a nonradioactive immunosorbent assay for p38alpha mitogen-activated protein kinase activity. *Anal Biochem* 406: 233-234.
- GU W, WUR, QIS, GUC, SIFAND CHEN Z. 2012. Synthesis and antibacterial evaluation of new N-acylhydrazone derivatives from dehydroabiatic acid. *Molecules* 17: 4634-4650.
- GUNDOGDU-HIZLIATESC, ALYURUKH, GOCMENTURK M, ERGUN Y AND CAVAS L. 2014. Synthesis of new ibuprofen derivatives with their *in silico* and *in vitro* cyclooxygenase-2 inhibitions. *Bioorg Chem* 52: 8-15.
- HE H, XIA H, XIA Q, REN Y AND HE H. 2017. Design and optimization of N-acylhydrazone pyrimidine derivatives as E. coli PDHc E1 inhibitors: Structure-activity relationship analysis, biological evaluation and molecular docking study. *Bioorg Med Chem* 25: 5652-5661.
- HERNÁNDEZ-VÁZQUEZ E, SALGADO-BARRERA S, RAMÍREZ-ESPINOSA JJ, ESTRADA-SOTO S AND HERNÁNDEZ-LUIS F. 2016. Synthesis and molecular docking of N'-arylidene-5-(4-chlorophenyl)-1-(3,4-dichlorophenyl)-4-methyl-1H-pyrazole-3-carbohydrazides as novel hypoglycemic and antioxidant dual agents. *Bioorg Med Chem* 24: 2298-2306.
- HERNÁNDEZ P, ROJAS R, GILMAN RH, SAUVAIN M, LIMA LM, BARREIRO EJ, GONZÁLEZ M AND CERECETTO H. 2013. Hybrid furoxanyl N-acylhydrazone derivatives as hits for the development of neglected diseases drug candidates. *Eur J Med Chem* 59: 64-74.
- JAGTAP VA, AGASIMUNDIN YS, JAYACHANDRAN E AND SATHE BS. 2011. *In vitro* anti-inflammatory activity of 2-amino-3-(substituted benzylidene-carbohydrazide)-4,5,6,7-tetrahydrobenzothiophenes. *J Pharm Res* 4: 378-379.
- JIN Y, TAN Z, HE M, TIAN B, TANG S, HEWLETT I AND YANG M. 2010. SAR and molecular mechanism study of novel acylhydrazone compounds targeting HIV-1 CA. *Bioorg Med Chem* 18: 2135-2140.
- JONES AM. 2017. Privileged Structures and Motifs (Synthetic and Natural Scaffolds). In: *Comprehensive Medicinal Chemistry III*. Elsevier, Oxford, UK, p. 116-152.
- KHALIL NA, AHMED EM, MOHAMED KO AND ZAITONE SAB. 2013. Synthesis of new nicotinic acid derivatives and their evaluation as analgesic and anti-inflammatory agents. *Chem Pharm Bull* 61: 933-940.
- KÜMMERLE AE ET AL. 2009. Studies towards the identification of putative bioactive conformation of potent vasodilator arylidene N-acylhydrazone derivatives. *Eur J Med Chem* 44: 4004-4009.
- LACERDA RB, DA SILVA LL, DE LIMA CK, MIGUEZ E, MIRANDA AL, LAUFER SA, BARREIRO EJ AND FRAGA CA. 2012. Discovery of novel orally active anti-inflammatory N-phenylpyrazolyl-N-glycinyld-hydrazone derivatives that inhibit TNF-alpha production. *PLoS ONE* 7: e46925.
- LI L, ZHANG Y, ZHANG J AND ZHENG A. 2013. Preparation method of articaine hydrochloride - CN102060840 B.
- LIN X, WANG M, ZHANG J AND XU R. 2014. p38 MAPK: a potential target of chronic pain. *Curr Med Chem* 21: 4405-4418.
- MOLDOVAN CM, ONIGA O, PÂRVU A, TIPERCIUC B, VERITE P, PÎRNĂU A, CRIȘAN O, BOJIȚĂ M AND POP R. 2011. Synthesis and anti-inflammatory evaluation of some new acyl-hydrazones bearing 2-aryl-thiazole. *Eur J Med Chem* 46: 526-534.
- OZADALI K, OZKANLI F, JAIN S, RAO PPN AND VELAZQUEZ-MARTINEZ CA. 2012. Synthesis and biological evaluation of isoxazolo[4,5-d]pyridazin-4-(5H)-one analogues as potent anti-inflammatory agents. *Bioorg Med Chem* 20: 2912-2922.
- PALACE-BERL F, JORGE SD, PASQUALOTO KFM, FERREIRA AK, MARIA DA, ZORZI RR, DE SÁ BORTOLOZZO L, LINDOSO JAL AND TAVARES LC. 2013. 5-Nitro-2-furfuriliden derivatives as potential anti-Trypanosoma cruzi agents: Design, synthesis, bioactivity evaluation, cytotoxicity and exploratory data analysis. *Bioorg Med Chem* 21: 5395-5406.
- PALLA G, PELIZZI C AND PREDIERI G. 1982. Conformational study on N-acylhydrazones of aromatic aldehydes by NMR spectroscopy. *Gazz Chim Ital* 112: 339-341.
- TIPERCIUC B, PÂRVU A, TAMAIAAN R, NASTASĂ C, IONUȚ I AND ONIGA O. 2013. New anti-inflammatory thiazolyl-carbonyl-thiosemicarbazides and thiazolyl-azoles with antioxidant properties as potential iNOS inhibitors. *Arch Pharm Res* 36: 702-714.
- ÜNSAL-TAN O, ÖZDEN K, RAUK A AND BALKAN A. 2010. Synthesis and cyclooxygenase inhibitory activities of some N-acylhydrazone derivatives of isoxazolo[4,5-d]pyridazin-4(5H)-ones. *Eur J Med Chem* 45: 2345-2352.
- ZARUBIN T AND HAN J. 2005. Activation and signaling of the p38 MAP kinase pathway. *Cell Res* 15: 11-18.
- ZHAI X, HUANG Q, JIANG N, WU D, ZHOU H AND GONG P. 2013. Discovery of hybrid dual N-acylhydrazone and diaryl urea derivatives as potent antitumor agents: Design, synthesis and cytotoxicity evaluation. *Molecules* 18: 2904-2923.

SUPPLEMENTARY MATERIAL

Figures: S1-S14.